Cancer Cell International

RESEARCH

Open Access

Overexpressed NEK2 contributes to progression and cisplatin resistance through activating the Wnt/β-catenin signaling pathway in cervical cancer

Jiang Haiye[1,2], Wang Xiangzhu[3], Zhang Yunfei[2], Gui Shumin[2], Ni Chang[2], Jiang Yaohui[2], Yin Heng[2] and Nie Xinmin[2*]

Abstract

Background Cervical cancer ranks as the fourth most common cancer among women, with cisplatin resistance posing a significant challenge to the long-term survival of patients.

Methods The roles of NEK2 in cervical cancer were examined through bioinformatics analysis. Transfection efficiency and molecular mechanisms were assessed using real-time quantitative polymerase chain reaction (qRT-PCR) and western blotting (WB). To evaluate cell functions, a series of assays, including cell counting kit-8 (CCK-8), wound healing, transwell, colony formation, and flow cytometry (FCM), were performed on HeLa, SiHa, and HeLa/DDP (cisplatin-resistant) cell lines.

Results We found that NEK2 is upregulated in cervical cancer tissues compared to normal tissues and is further elevated in cisplatin-resistant cervical cancer compared to cisplatin-sensitive cases. The overexpression of NEK2 is associated with enhanced cancer progression, poorer prognosis, and increased cisplatin resistance in cervical cancer patients. Notably, in the presence of cisplatin, the knockdown of NEK2 inhibited cell viability, proliferation, migration, invasion, and G2/M phase arrest in cervical cancer cells, while also enhancing the sensitivity of cisplatin-resistant cervical cancer cells through the inactivation of the Wnt/β-catenin signaling pathway.

Conclusions NEK2 is upregulated in cervical squamous cell carcinoma (CESC) compared to normal tissues and exhibits higher levels in cisplatin-resistant CESC than in sensitive counterparts, correlating with disease progression and poor prognosis. Thus, NEK2 is implicated in the cisplatin resistance of CESC via the activation of the Wnt/β-catenin signaling pathway, suggesting its potential as a prognostic marker and a novel target for the diagnosis and treatment of cisplatin-resistant CESC.

Keywords NEK2, Cervical cancer, Cisplatin resistance, Progression, Wnt/β-catenin

*Correspondence:
Nie Xinmin
niexinmin7440@sina.com
[1]School of Medicine, Hunan Normal University, Changsha 410013, China
[2]Department of Laboratory Medicine, The Third Xiangya Hospital, Central South University, Changsha 410013, China
[3]Department of Conservative and Endodontic Dentistry, Xiangya School and Hospital of Stomatology, Hunan Key Laboratory of Oral Health Research, Central South University, Changsha 410008, China

Background

Cervical cancer is a malignant disease that originates from the cervix uteri, which originates from a lot of carcinogenic agents [1]. Cervical squamous cell carcinoma (CESC) accounts for the primary pathological type of cervical cancer and is the fourth most frequently diagnosed gynecological cancer among females. Meanwhile, CESC represents the fourth cancer-related mortality in females worldwide [2]. It was estimated that 604,127 new cases and 341,831 women died because of CESC in 2020 [2]. As the first generation platinum chemotherapeutics, cisplatin (DDP) plays a vital role in locally advanced and recurred cervical cancer [3]. DDP concurrent with radiotherapy after surgery is the standard treatment commonly applied to cervical cancer patients [4]. However, chemotherapy for cervical cancer usually fails because of the inherent or acquired resistance to DDP [5]. Hence, it is essential to discover the underlying mechanism of DDP resistance in cervical cancer.

As a serine/threonine centrosomal kinase, NIMA-related kinase 2 (NEK2) is a central constituent of the human centrosome, which plays a pivotal role in mitosis, especially in spindle formation and chromosome segregation [6]. *NEK2* was regarded as an important oncogene in various tumors [7]. It was discovered that NEK2 was overexpressed in a wide variety of human cancers, including cervical cancer [8], ovarian cancer [9], breast cancer [10], prostate cancer [11], head and neck squamous cell carcinoma [12], and so on. Upregulated *NEK2* levels can lead to chromosome instability and aneuploidy, which will ultimately promote carcinogenesis [13]. Meanwhile, it was discovered that upregulated *NEK2* contributed to cisplatin-based chemotherapy resistance [12, 14]. However, the roles and underlying mechanisms of *NEK2* in cisplatin resistance in CESC have not been investigated.

It was confirmed that NEK2 is highly expressed in cervical cancer cells compared to normal cervical epithelial cells, and upregulated NEK2 inactivates the Hippo pathway to advance the proliferation of cervical cancer cells [15]. However, the pathogenic effect of upregulated NEK2 on cisplatin resistance in cervical cancer has not been studied. Previous research has demonstrated that NEK2 activates the Wnt/β-catenin signaling pathway via Wnt1 to drive oncogenesis and radioresistance in cervical cancer, indicating that NEK2 may be a promising target for the radiosensitization of cervical cancer [16]. However, the pathogenic mechanism of overexpressed NEK2 on cisplatin resistance in cervical cancer remains unclear. It was reported that high expressed NEK2 was related to multidrug resistance of head and neck squamous cell carcinoma, and high NEK2 contributed to cisplatin-based chemotherapy resistance in nasopharyngeal carcinoma [17, 18]. In summary, the above studies prove that overexpression of NEK2 may be related to the pathogenesis of cervical cancer, and NEK2 may be a key gene related to tumor drug resistance. However, the effect and mechanism of overexpression of NEK2 on cisplatin resistance of cervical cancer are still unclear.

The canonical Wnt/β-catenin signaling pathway plays a vital role in regulating plenty of physiological and pathological processes, such as cell proliferation, migration, invasion, and so on [19]. β-catenin is a multipurpose protein that plays essential roles in the Wnt/β-catenin signaling pathway and centrosome segregation [20]. Various research indicated that NEK2 can interact with β-catenin to prevent β-catenin degradation and enhance the progressive properties of cancer cells [21, 22]. It is reported that the disordered Wnt/β-catenin signaling pathway correlated with tumorigenesis in several kinds of tumors, such as ovarian cancer, breast cancer, and hepatocellular carcinoma (HCC) [23, 24]. Meanwhile, it was discovered that Wnt/β-catenin signaling played an important part in cisplatin resistance by influencing DNA damage repair [25]. Nevertheless, there is limited evidence on the combinatorial effect of NEK2 with cisplatin resistance in CESC. Furthermore, the relationship of NEK2 with the Wnt/β-catenin signaling pathway on cisplatin resistance in CESC is poorly understood.

The purpose of our study is to screen out a clinically valuable gene target to predict and treat cisplatin resistance in CESC and elucidate the underlying mechanism of oncogenesis and inducing cisplatin resistance.

Materials and methods

Data extraction

We filtrated the datasets from the Gene Expression Omnibus (GEO) database associated with CESC and downloaded two datasets (GSE9750 (including 24 normal samples and 33 CESC samples) and GSE63514 (including 24 normal samples and 28 CESC samples)), and then we filtrated the datasets from GEO database associated with CESC and cisplatin resistance and obtained two datasets (GSE56363 (including 12 therapy-sensitive CESC samples and 9 intrinsic resistant CESC samples). We downloaded CESC datasets (including 3 normal samples and 306 CESC samples) from the Cancer Genome Atlas (TCGA) database (https://portal.gdc.cancer.gov/), including gene expression data and clinical information. The detailed clinical characteristics of the CESC patients from TCGA are listed in Table 1. GSE9750 and GSE56363 were used as training groups, while GSE63514 were used as testing groups. Human CESC tissue was from a woman with CESC aged 32, and normal cervix tissue was from a healthy woman aged 37.

Data analysis

We employed the 'limma' R package to read transcriptome profiling information and microarray data and

Table 1 Characteristics of the study participants

Variable		CESC			Normal	Total	*P*-value
		306			3	309	
Age	Mean (IQR)	47(39,57)			55(48,62)		0.44 [a]
Sex	Female	306(100.0%)			3(100.0%)	309(100.0%)	> 0.99 [b]
	Male	0(0.0%)			0(0.0%)	0(0.0%)	
Smoking	Yes	263(85.9%)			2(66.7%)	265(85.8%)	0.37 [b]
	No	43(14.1%)			1(33.3%)	44(14.2%)	
Pregnancy	Yes	250(81.7%)			2(66.7%)	252(81.6%)	> 0.99 [b]
	No	17(5.6%)			0(0%)	17(5.5%)	
	Unknown	39(12.7%)			1(33.3%)	40(12.9%)	
Grade	G1	18(5.9%)					
	G2	136(44.4%)					
	G3	121(39.5%)					
	G4	1(0.3%)					
	GX	30(9.8%)					
Primary tumor size	T1	140(45.8%)					
	T2	72(23.5%)					
	T3	22(7.2%)					
	T4	10(3.3%)					
	TX	62(20.3%)					
Lymph node status	N0	135(44.1%)					
	N1	58(19.0%)					
	NX	113(36.9%)					
Metastasis status	M0	135(44.1%)					
	M1	10(3.3%)					
	MX	161(52.6%)					
Tumor stage	I	163(53.3%)					
	II	70(22.9%)					
	III	46(15.0%)					
	IV	21(6.9%)					
	X	6(2.0%)					
Chemotherapy		Complete response	Partial response	Unknown			
	Cisplatin	64(58.2%)	18(16.4%)	28(25.5%)		110	
	Carboplatin	0(0%)	4(66.7%)	2(33.3%)		6	
	Others	12(50.0%)	5(20.8%)	7(29.2%)		24	
	Unknown	68(41.0%)	7(10.6%)	91(54.8%)		166	

a T test; b Pearson's Chi Square test/Fisher's exact analysis

normalize the gene expression levels of each sample for differential analysis. We gained the differential expression genes (DEGs) of each file with P-values and logFC values with t-tests. We filtered the DEGs with |log2foldchange| > 1 and adjP < 0.05.

IC_{50} of cisplatin in cervical cancer is defined as half the maximal inhibitory concentration of cisplatin to cervical cancer cell lines, which refers to the concentration of cisplatin that can inhibit the viability of cervical cancer cells to 50% under experimental conditions in this work. We calculated IC_{50} based on the GraphPad method. As follows: First, three multiple holes were set up in each group. After the experiment was completed, absorbance (OD) at 450 nm was measured by enzyme marker (Tecan, Switzerland) for the blank control group (Ab), positive control group (Ac), and experiment group treated with different concentrations of cisplatin (As). The mean OD value of each group was calculated respectively, and the survival rate was calculated by the formula as follows: [(As-Ab)/(Ac-Ab)]*100%. Second, fill the GraphPad table with the survival rate and transform the concentration of cisplatin to log10 (standard) in the analysis. Subsequently, the log inhibitor VS normalized response-variable slope function was used to calculate the survival rate so as to obtain the corresponding IC_{50} value. Finally, the curve of the relative change of cisplatin concentration and cell viability was fitted.

LASSO regression analysis was used to extract the key dominant factors in a subset. Kaplan-Meier survival analysis was used to evaluate the survival condition of a crowd based on current information, which was presented by the overall survival (OS) and progression-free

survival (PFS) curve. The receiver operating characteristic (ROC) curve was used to estimate the performance of a disaggregated model. Gene ontology (GO) analysis was used to achieve functional classification of genes or proteins based on sequence information. Kyoto Encyclopedia of Genes and Genomes (KEGG) analysis is mainly aimed at the analysis of metabolic pathways in organisms based on gene expression information. Gene set enrichment analysis (GSEA) is used to identify whether a predefined set of genes exhibits significant and consistent differences between two biological states.

Cell lines and culture

HeLa and SiHa cell lines were purchased from Shanghai Meixuan Biological Science and Technology LTD (Shanghai, China), HeLa/DDP (cisplatin-resistant) cell line was purchased from TONGPAI BIOTECHNOLOGY CO., LTD (Shanghai, China), and human normal cervical epithelial cell lines (HUCEC) was provided from Dr. Li. HeLa, SiHa and HeLa/DDP cell line have recently been authenticated by detecting STR and Amelogenin loci. All of the cell lines have recently been tested for mycoplasma contamination. All the cell lines were cultured in 1640 medium (GIBCO, Grand Island, NY, USA) appended with 10% fetal bovine serum (FBS) (Hyclone, Logan, UT, USA) and 1% penicillin-streptomycin (Hyclone). All cells were cultured in an incubator with 5% CO_2 and humidification at 37 ℃.

Plasmid assembling and cell transfection

We synthesized the full-length *NEK2* cDNA (NM_002497) from cells and then sub-cloned it into the vector (pEGFP-N1ZB04981) to construct the pcDNA-*NEK2* overexpression (OE-*NEK2*) plasmid (Sangon Biotech, Shanghai, China). shRNA sequences targeting *NEK2* were synthesized and then cloned into hU6/EGFP/puro plasmid (Genechem, Shanghai, China). Transient transfections of all plasmids were performed using Lipofectamine 8000 reagent (Beyotime, Shanghai, China). All cell transfections were based on the manufacturer's instructions. The sequences of these nucleic acids are listed in Supplementary Table 1.

Extracting RNA and qRT-PCR

Total RNA was extracted using TRIzol Reagent (Simgen, Hangzhou, China). The concentration and purity of total RNA were determined by a micro-spectrophotometer (Allsheng, Hangzhou, China). CDNA was synthesized using the M-MuLV First Strand cDNA Synthesis Kit (Sangon Biotech). The real-time quantitative polymerase chain reaction (qRT-PCR) was performed using 2× SG Fast qPCR Master Mix (Sangon Biotech) and Roche LightCycler® 96 (Roche, Basel, Switzerland). GAPDH was used as an internal reference gene. The results were analyzed by the 2-ΔΔCt method. All primer sequences are listed in Supplementary Table 1.

Extracting protein and Western blot

The cells were washed with phosphate-buffered saline (PBS, Meilunbio) and then lysed in RIPA buffer (Cwbio, Beijing, China). To remove any cell debris, the lysates were centrifuged at 12,000 g for 15 min at 4 °C. An equal amount of total protein lysates (20 μg) was subjected to 8–10% sodium dodecyl sulfate-polyacrylamide gel electrophoresis (SDS-PAGE) and subsequently transferred onto an NC membrane (Amresco, Solon, OH, USA). Following blocking to prevent nonspecific binding, the membranes were incubated with a primary antibody overnight at 4 °C, and then with a secondary antibody (1:10000 dilution; Biodragon, Suzhou, China) for 1 h at room temperature. The bands were visualized using an automatic chemical exposure analysis system complex 2000. Primary antibodies were as follows: NEK2 (1:1,000; Proteintech, Wuhan, China), GAPDH (1:3,000; Affinity, Changzhou, China), C-Myc (1:1,000; Proteintech), β-catenin (1:1,000; Proteintech), β-Tubulin (1:3,000; Affinity). The experiments were independently repeated in triplicate.

Cell counting kit-8 (CCK-8) assay

To perform the cell viability assay, 1×10^3 HeLa and SiHa shRNA transfected cells in 100 μL of complete culture media were seeded in 96-well plates and then treated with different concentrations of cisplatin for 24 h. Cell viability was measured using a CCK-8 assay (TOPSCIENCE, Shanghai, China) following the manufacturer's instructions. After incubating the cells at 37 °C for 4 h, the absorbance was measured at 450 nm using a microplate reader (Tecan, Männedorf, Switzerland). The experiments were independently repeated in triplicate.

Colony formation assay

HeLa and SiHa shRNA transiently transfected cells were counted and 100 cells were inoculated into 6 cm plates and treated with 2 μM cisplatin, which were cultured in an incubator with 5% CO_2 and humidification at 37∘C for two weeks. The cells were then washed with PBS fixed with 4% paraformaldehyde (Biosharp, Hefei, China) and stained with 0.1% crystal violet (Beyotime), and the experiments were independently repeated in triplicate.

Wound healing assay

HeLa and SiHa shRNA transiently transfected cells were seeded in six-well plates at a density of 2.5×10^6 cells per well. Once the cells reached 100% confluency, a straight wound was created by using 200-μL tips, and the cells were then incubated in a medium containing 1% FBS and 2 μM cisplatin. The closure of the wound was monitored

at 0 and 48 h, and the experiments were independently repeated in triplicate.

Transwell assay

The upper chambers (LABSELECT, Hefei, China) of a 24-well plate were coated with Matrigel (Corning Bioscience, New York, NY, USA) in a non-serum medium and incubated for 2 h at 37 °C. Next, 1×10^5 transfected cells were seeded in the upper chamber using serum-free 1640, while the lower chamber was filled with culture medium containing 10% FBS and 2 μM cisplatin. After 48 h, the invaded cells were fixed with 4% paraformaldehyde and stained with crystal violet. The cells that had invaded through the membrane were counted and visualized using a microscope (Zeiss, Oberkochen, Germany); 5 fields were selected to count the cells. The experiments were independently repeated in triplicate.

Flow cytometry (FCM) assay

The cell cycle assay kit (Elabscience, Wuhan, China) was used to evaluate the cell cycle following the manufacturer's protocol. Briefly, HeLa and SiHa shRNA transiently transfected cells treated with 2 μM cisplatin for 24 h were harvested and treated with absolute ethyl alcohol and RNaseA Reagent in turn and stained with PI, respectively. Changes in cell cycle were detected based on DNA content and were measured using BD FORTESSA (Becton, Dickinson and Company, Franklin Lake, NJ, USA). PI was detected at 575 nm. The experiments were independently repeated in triplicate.

Statistical analysis

Data were analyzed by SPSS 25.0 and displayed as mean ± SD. The statistical significance of differences was evaluated by two-tailed Student's t-test or two-way ANOVA. Statistical analyses were performed using Prism software (GraphPad Software). $P < 0.05$ were considered statistically significant.

Results

NEK2 was the key gene contributing to platinum drug resistance in CESC

To gain a comprehensive understanding of the distribution of DEGs, we generated volcano maps (Fig. 1A and C) and heat maps (Fig. 1B and D) specifically depicting the DEGs in GSE9750 and GSE56363, respectively. We found that there were 706 genes upregulated in GSE9750, and 122 genes upregulated in GSE56363; meanwhile, there were 620 genes down-regulated in GSE9750, and 225 genes upregulated in GSE56363, respectively. To screen out the common genes both upregulated and down-regulated in GSE9750 and GSE56363, we conducted Venn diagrams and found 32 genes upregulated both in GSE9750 and GSE56363 (Fig. 1E), and 13 genes down-regulated both in GSE9750 and GSE56363 (Fig. 1F). On account of the typical 45 DEGs, we implemented GO enrichment analysis (Fig. 1G and I), and discovered the biological functions of these 45 co-expression DEGs mainly enriched in chromosome segregation, nuclear division and positive regulation of cell cycle process. We also carried out KEGG enrichment analysis (Fig. 1J and K), and found the pathways of these 45 co-expression DEGs mainly enriched in drug metabolism, platinum drug resistance, and Fanconi anemia pathway.

In order to gain the key pathogenic genes of CESC and intrinsic resistant CESC, firstly, we implemented protein-protein interaction (PPI) analysis of all 45 co-expression DEGs to gain PPI network in different ways (Fig. 2A), and drawn a node network diagram which convey the interaction of each gene and all of the genes were upregulated in CESC (Fig. 2B). We further searched cluster network based on the node network above, and obtained two cluster networks, which indicated the genes with close relations in a cluster (Fig. 2C). We conducted hub gene analysis of the PPI network, which allowed us to obtain 15 core genes of the network (Fig. 2D). We also carried out GeneMANIA network analysis based on the 15 core genes, with which we could know the interaction network and functions of core genes, which indicated us the functions of the core genes mainly focus on mitotic nuclear division and mitotic sister chromatid segregation (Fig. 2E). We implemented GO analysis to study the functions of the core genes (Fig. 2F and G), which mainly focus on nuclear division, chromosome segregation and mitotic sister chromatid segregation. Moreover, we conducted a KEGG analysis to reveal the pathways related to the core genes (Fig. 2H and I), which revealed that the core genes had an impact on CESC's platinum drug resistance. We then filtered the core genes using Lasson regression analysis to obtain the characteristic genes of CESC and therapy-resistant CESC. We acquired 4 characteristic genes in GSE9750 (Fig. 2J and K), and 4 characteristic genes in GSE56363 (Fig. 2L and M), respectively. Therewith, we did a Venn analysis between 4 characteristic genes in GSE9750 and in GSE56363 (Fig. 2N) and gained a gene *NEK2*, which was the key gene related to both CESC and intrinsic resistant CESC, through influencing nuclear division and platinum drug resistance.

NEK2 is upregulated in CESC and intrinsic resistant CESC compared to normal tissues and sensitive CESC, respectively, and is associated with tumor growth, cisplatin resistance, and worse prognosis in CESC

We conducted the differential expression analysis of *NEK2* in pan-cancers and found NEK2 was overexpressed in various carcinomas; *NEK2* was significantly upregulated in CESC based on TCGA ($P < 0.01$, Fig. 3A and B). Meanwhile, we implemented a comparative

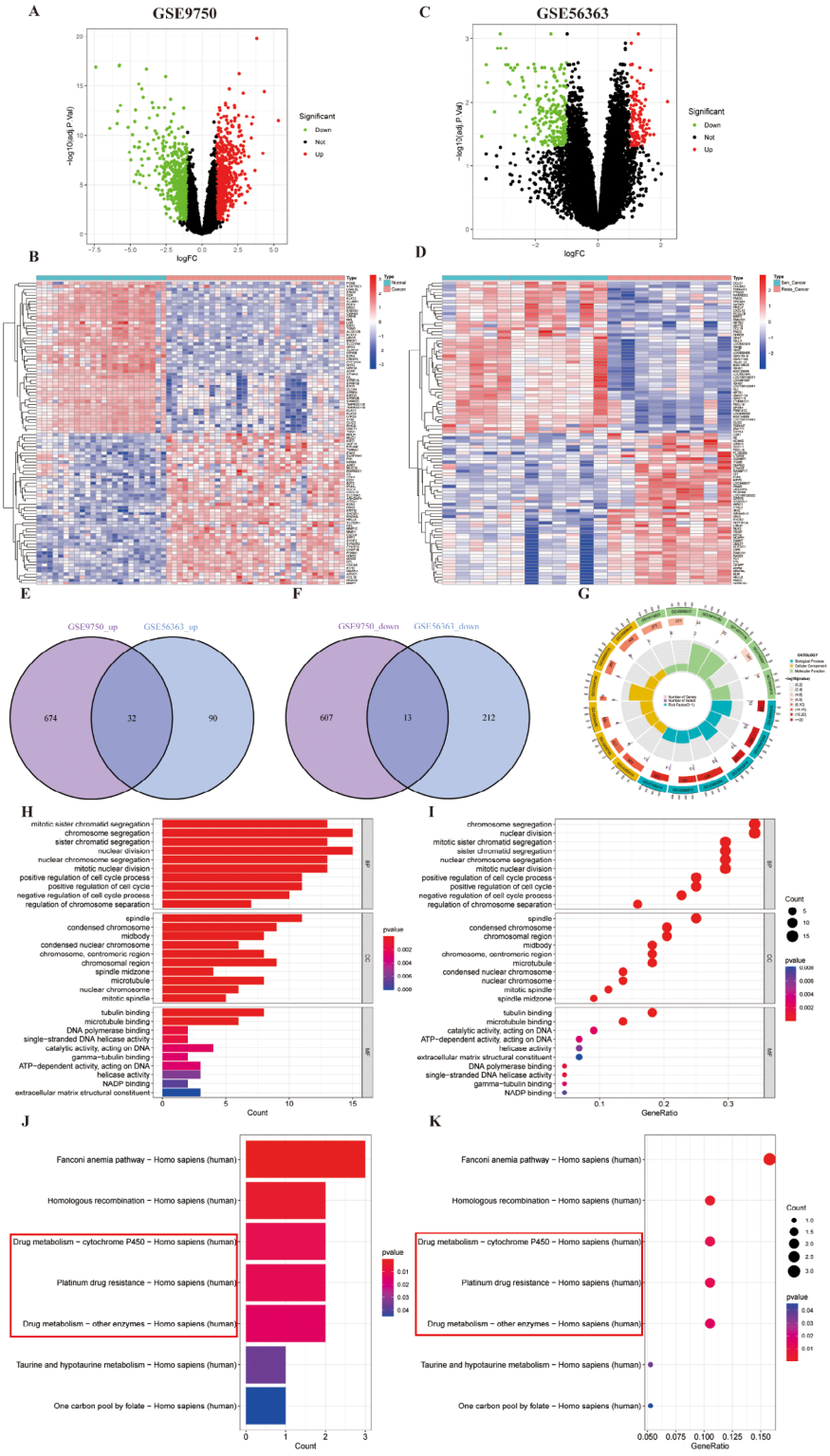

Fig. 1 Co-expression differential genes in CESC and intrinsic resistance CESC and their GO and KEGG analysis. (**A**) Volcano plot of DEGs of GSE9750. (**B**) Heatmap of top 50 DEGs of GSE9750. (**C**) Volcano plot of DEGs of GSE56363. (**D**) Heatmap of top 50 DEGs of GSE56363. (**E**) The Venn diagram of DEGs is both upregulated in GSE9750 and GSE56363. (**F**) The Venn diagram of DEGs is both down-regulated in GSE9750 and GSE56363. (**G**) The circle diagram, (**H**) the barplot, and (**I**) the bubble plot of GO analysis based on 45 co-expression DEGs in GSE9750 and GSE56363. (**J**) The barplot (**K**) is the bubble plot of KEGG analysis based on 45 co-expression DEGs in GSE9750 and GSE56363

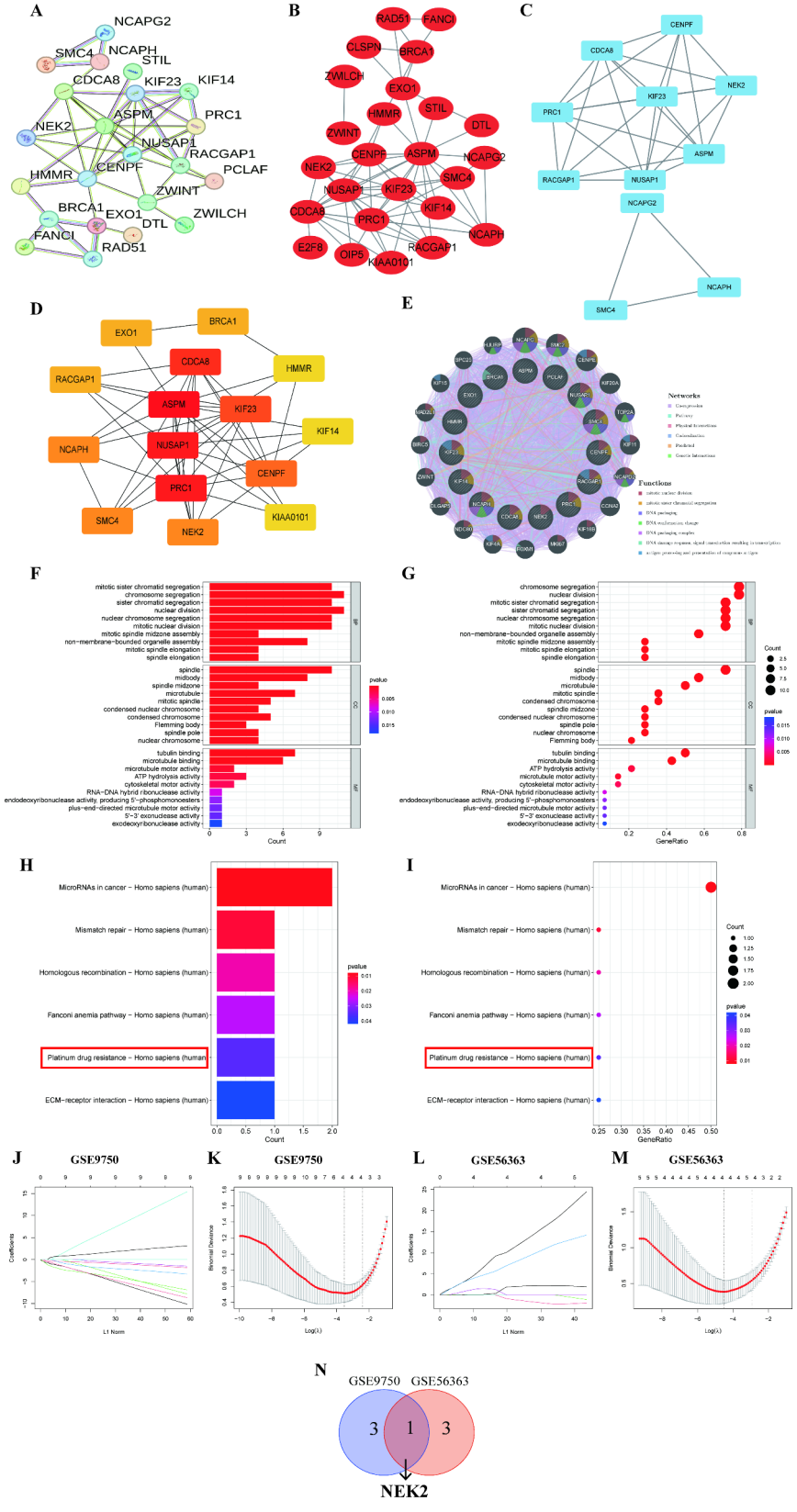

Fig. 2 (See legend on next page.)

(See figure on previous page.)

Fig. 2 NEK2 is the key pathogenic gene relating to CESC and intrinsic resistant CESC through influencing nuclear division and platinum drug resistance. (**A**) The protein-protein interaction (PPI) network based on PPI analysis of all 45 co-expression DEGs, each circle represents a single gene, and the tie line in different colors means two genes interacted in different ways. (**B**) In the node network diagram of all 45 co-expression DEGs, the red color of each gene means the gene is upregulated in CESC. (**C**) Two cluster networks based on the node network. (**D**) In the hub gene analysis of the PPI network, the depth of the color indicates the importance of the gene, and the darker color means the more important the gene. (**E**) GeneMANIA network analysis based on the 15 core genes, the inner circle represents the hub genes while the outside circle represents the genes related to the hub genes; the tie line in different colors means two genes interacted in different ways, the different color of pies in a circle represents different functions. (**F**) The barplot and (**G**) the bubble plot of GO analysis based on 15 core genes. (**H**) The barplot, (**I**) the bubble plot of KEGG analysis based on 15 core genes

analysis of *NEK2* expression level between CESC and normal samples based on GSE9750 and GSE63514 and found *NEK2* was significantly overexpressed in CESC ($P < 0.001$, Fig. 3C and E). We also carried out a comparison of *NEK2* between intrinsic resistant CESC and sensitive CESC based on GSE56363, and found *NEK2* was significantly overexpressed in intrinsic resistant CESC ($P < 0.001$, Fig. 3D). What is more, the expression level of *NEK2* was found to be a valuable predictor of CESC and intrinsic resistant CESC, as indicated by ROC curve based on GSE9750 (area under the curve (AUC) = 0.965, Fig. 3F), GSE56363 (AUC = 0.991, Fig. 3G) and GSE63514 (AUC = 0.900, Fig. 3H). Survival analysis indicated that patients with high levels of NEK2 did not exhibit significantly reduced overall survival time ($P = 0.738$, Fig. 3I) and progression-free survival time ($P = 0.082$, Fig. 3J), while high expression level of *NEK2* related to shorter progression-free survival time (Fig. 3J). ROC curve indicated that the expression level of *NEK2* could not effectively predict a survival time in 5 years (all AUC < 0.6, Fig. 3K).

To study the association of *NEK2* with clinical characteristics, we conducted the correlation analysis of *NEK2* expression with age ($P = 0.83$, Fig. 4A), grade (Fig. 4B), stage (Fig. 4C), primary tumor size (T) (Fig. 4D), lymph node metastasis (N) ($P = 0.24$, Fig. 4E), distant metastasis (M) ($P = 0.12$, Fig. 4F) and cisplatin response ($P = 0.00072$, DDP_Response) (Fig. 4G) in CESC. We also drew the heatmap of different clinical characteristics in high and low *NEK2* expression groups and found the expression level of *NEK2* was correlated with grade ($P < 0.001$, Fig. 4H) and DDP_Response ($P < 0.01$, Fig. 4H), which was consistent with the results above. In terms of OS, we developed a nomogram (Fig. 4I) to assess the prognostic value of *NEK2* expression level and clinical characteristics, as well as a calibration graph (Fig. 4J). Moreover, based on *NEK2* expression level and clinical characteristics, we implemented independent prognostic analysis and found *NEK2* could not be used as an independent prognostic factor in univariate COX analysis ($P = 0.622$, Fig. 4K) and multivariate COX analysis ($P = 0.074$, Fig. 4L). However, we found lymph node metastasis could be used as an independent prognostic factor in univariate COX analysis ($P < 0.001$, Fig. 4K) and multivariate COX analysis ($P = 0.01$, Fig. 4L); we also found cisplatin resistance could be used as an independent prognostic factor in univariate COX analysis ($P < 0.001$, Fig. 4K) and multivariate COX analysis ($P = 0.025$, Fig. 4L). These results indicated that *NEK2* was observably correlated with grade, primary tumor size, and cisplatin resistance, while lymph node metastasis and cisplatin resistance could be used as independent prognostic factors.

GO, KEGG, and GSEA analysis of *NEK2*-related genes in CESC based on TCGA

To study the functions and pathways of *NEK2*-related genes, we analyzed the DEGs based on the expression level of *NEK2* and drew the heatmap for the top 50 DEGs (Fig. 5A). Meanwhile, we conducted GO analysis based on the DEGs and investigated the functions of the DEGs mainly focused on axoneme assembly, microtubule – based movement and cell motility (Fig. 5B and D). Furthermore, we performed KEGG analysis based on the DEGs and found the pathways of the DEGs mainly concentrated on motor proteins and neuroactive ligand – receptor interaction (Fig. 5E and F). We also implemented GSEA enrichment analysis to discover the differential biological functions or pathways associated with high and low *NEK2* expression groups. The results conveyed that the functions of the low *NEK2* expression group are principally related to the down-regulating of epidermal cell differentiation, keratinization, and immunoglobulin complex (Fig. 5G). The pathways of the low *NEK2* expression group were predominantly associated with autoimmune thyroid disease, graft-versus-host disease, and ribosome (Fig. 5H). These findings hinted that *NEK2* may promote CESC tumorigenesis and cisplatin resistance by influencing cell movement and the immune microenvironment.

Downregulated NEK2 inhibits cell proliferation, migration, invasion, and cell cycle in CESC cells and restrains cisplatin resistance through Wnt/β-catenin pathway inactivation in cisplatin-resistant CESC cells

To study the differential expression of NEK2 in CESC and normal cervical cell lines, we detected *NEK2* mRNA and protein expression in HUCEC, HeLa, and SiHa cell lines and discovered *NEK2* were significantly overexpressed in HeLa and SiHa cells compared to HUCEC cells both in mRNA (Fig. 6A) and protein (Fig. 6B) levels. Based on the THPA (https://www.proteinatlas.org) proteomi c data website, we compared the differential expression

of NEK2 in human CESC tissue and normal cervix tissue; the results indicated NEK2 was upregulated in human CESC tissues than normal cervix tissue (Fig. 6C), human CESC tissue was from a woman with CESC aged 32, and normal cervix tissue was from a healthy woman aged 37. To assess the functional roles of NEK2 in CESC, we constructed *NEK2*-knockdown and *NEK2*-overexpression cell models with HeLa and SiHa cells. Results showed transfection with *NEK2*-knockdown (shNEK2) plasmid significantly decreased *NEK2* mRNA (Fig. 6D) and protein (Fig. 6E) expression levels compared to the shRNA-NC (shNC) groups in HeLa and SiHa cells. On the contrary, transfection with *NEK2*-overexpression (OE-NEK2) plasmid significantly increased *NEK2* mRNA (Fig. 6F) and protein (Fig. 6G) expression levels compared to the Vector groups in HeLa and SiHa cells. The results suggested that we successfully constructed *NEK2*-knockdown and *NEK2*-overexpression cell models using HeLa and SiHa cells.

Based on CCK-8 assays, we discovered that silencing of *NEK2* significantly reduced the cell viability of HeLa (Fig. 6H) and SiHa (Fig. 6I) cells at the concentration gradient of cisplatin, while overexpression of *NEK2* significantly increased the cell viability of HeLa (Fig. 6J) and SiHa (Fig. 6K) cells at concentration gradient of cisplatin. Based on wound healing assays, we found that knockdown of NEK2 and further treatment with cisplatin significantly decreased cell migration compared to shNC groups in both HeLa ($P<0.05$, Fig. 6L) and SiHa ($P<0.05$, Fig. 6M) cells. The results from transwell assays revealed that silencing *NEK2* and further treatment with cisplatin significantly decreased invasive cell numbers compared to shNC groups in both HeLa ($P<0.01$) and SiHa ($P<0.05$) cells (Fig. 6N). The results of colony formation assays indicated that silencing *NEK2* and further treatment with cisplatin could significantly inhibit cell proliferation in both HeLa ($P<0.05$) and SiHa ($P<0.05$) cells (Fig. 6O). Furthermore, results from the FCM assays revealed that the knockdown of *NEK2* and further treatment with cisplatin promoted cell cycle arrest in the G1/S phase and inhibited cell cycle arrest in the G2/M phase in both HeLa and SiHa cells (Fig. 6P). These findings suggest that NEK2 conferred cisplatin resistance and played a vital role in regulating cell viability, proliferation, migration, invasion, and cell cycle in CESC in vitro.

To study the role of NEK2 in cisplatin-resistant CESC cells, we examined *NEK2* mRNA and protein expression in HeLa and HeLa/DDP cells. We discovered *NEK2* was overexpressed in HeLa/DDP cells compared to HeLa cells both in mRNA ($P<0.05$, Fig. 7A) and protein ($P<0.01$, Fig. 7B) levels. We constructed *NEK2*-knockdown cell models in HeLa/DDP cells. Results showed transfection with shNEK2 plasmid significantly decreased *NEK2* mRNA ($P<0.05$, Fig. 7C) and protein ($P<0.01$, Fig. 7D) expression levels compared to shNC group. Furthermore, we detected the cell viability and cisplatin IC_{50} of HeLa and HeLa/DDP cells using CCK-8, and found that cisplatin IC_{50} of HeLa/DDP cells was 5 times larger than HeLa cells (Fig. 7E). Transfection with shNEK2 decreased cisplatin IC_{50} of HeLa/DDP cells, and increased HeLa/DDP cells' sensitivity to cisplatin (Fig. 7F). Cell proliferation analysis indicated transfection with shNEK2 decreased the cell cloning numbers of HeLa/DDP cells, and increased HeLa/DDP cells' sensitivity to cisplatin ($P<0.01$, Fig. 7G). It has been discovered that NEK2 could promote oncogenesis and radioresistance through the Wnt/β-catenin signaling pathway in cervical cancer [26]. A review of the BioGRID database (https://downloads.thebiogrid.org/BioGRID) suggested that MYC potentially interacted with NEK2. We hypothesize that NEK2 could facilitate cisplatin resistance in CESC through the Wnt/β-catenin signaling pathway. The variation in Wnt/β-catenin proteins prompted that knockdown or overexpression of *NEK2* changed the activity of the Wnt/β-catenin signaling pathway in the HeLa/DDP cells with cisplatin treatment (Fig. 7H and I). Knockdown of *NEK2* and cisplatin treatment resulted in decreased protein expression levels of β-Catenin ($P<0.001$, Fig. 7H) and C-Myc ($P<0.01$, Fig. 7H) in HeLa/DDP cells. On the contrary, overexpression of *NEK2* and cisplatin treatment promoted protein expression of β-Catenin ($P<0.01$, Fig. 7I) and C-Myc ($P<0.001$, Fig. 7I) in HeLa/DDP cells. Taken together, these data suggest that NEK2 drove cisplatin resistance through Wnt/β-catenin pathway activation in cisplatin-resistant CESC cells.

Discussion

This study processed a large number of clinical specimens and data by means of bioinformatic analysis without assuming the scope of specific key tumor pathogenic genes and discovered that NEK2 may be the key gene leading to cervical cancer and cisplatin resistance. Subsequently, the study used in vitro experiments to verify the carcinogenic function of NEK2 on cervical cancer pathogenesis and cisplatin resistance. This research discovered that upregulation of NEK2 could promote cervical cancer tumorigenesis and cisplatin resistance by activating the Wnt/β-catenin signaling pathway.

CESC is the fourth most common carcinoma in females and is the leading cause of death among malignancies for women worldwide [27]. Surgery followed by cisplatin-centered chemotherapy is the standard therapy for CESC patients. However, the frequent emergence of drug resistance limits the efficacy of anti-cancer therapies, which remains the major obstacle to the long-term survival of CESC patients [28]. The present research discovered that NEK2 is the key gene modulating cisplatin resistance in CESC through activation of the Wnt/β-catenin signaling

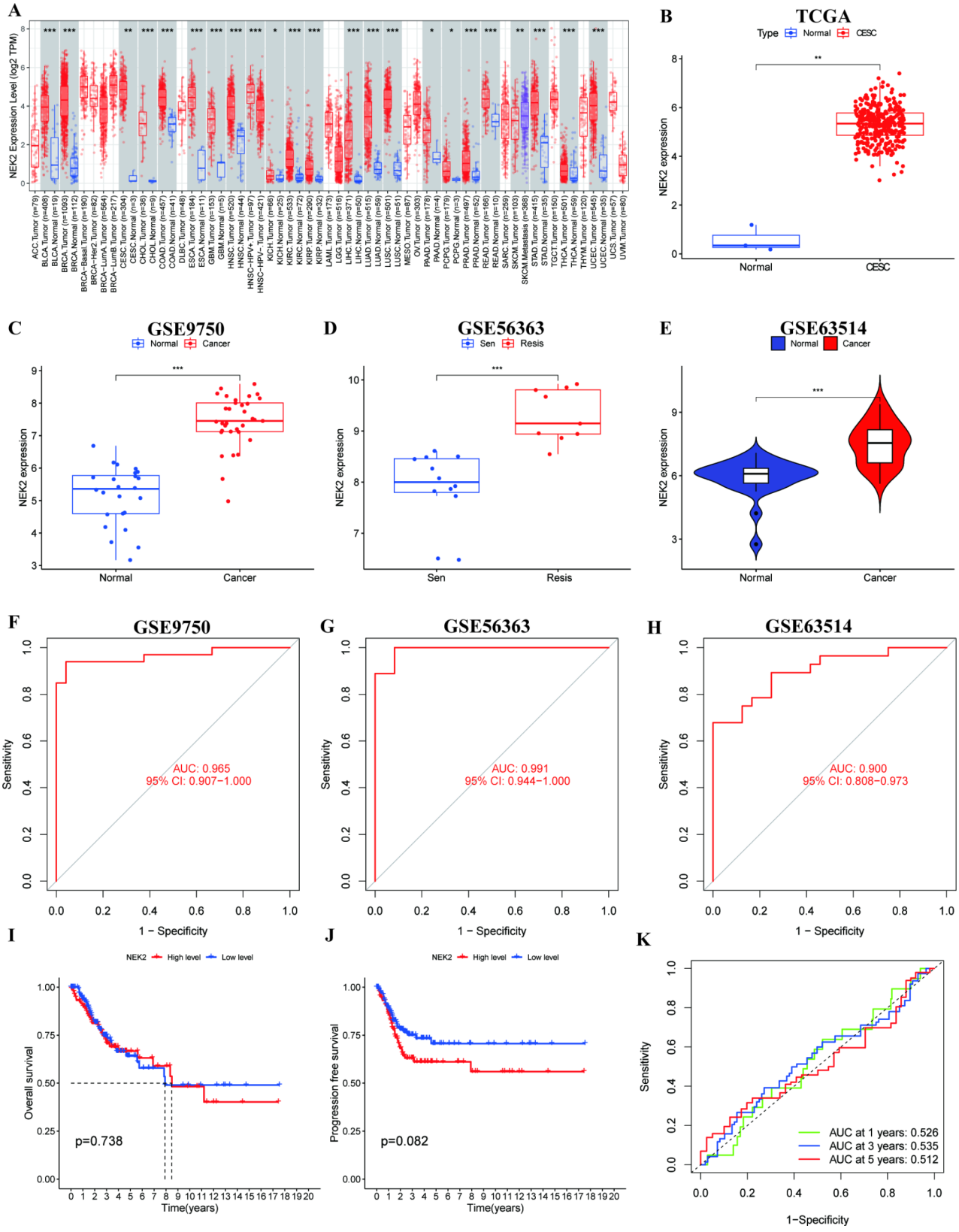

Fig. 3 (See legend on next page.)

(See figure on previous page.)

Fig. 3 NEK2 is upregulated in CESC and intrinsically resistant CESC compared to normal tissues and sensitive CESC, and it is associated with a worse prognosis. (**A**) The differential expression analysis of NEK2 in pan-cancers. (**B**) The boxplot of differential expression of NEK2 in CESC compared to normal samples based on TCGA. (**C**) The boxplot of differential expression of NEK2 in CESC compared to normal samples based on GSE9750. (**D**) The boxplot of differential expression of NEK2 in intrinsic resistance CESC compared to sensitive CESC samples based on GSE56363. (**E**) The violin plot of differential expression of NEK2 in CESC compared to normal samples based on GSE63514. The ROC curve for the predictive value of NEK2 is based on GSE9750 (**F**), GSE56363 (**G**), and GSE63514 (**H**). (**I**) The Kaplan-Meier curve for overall survival of patients with high and low levels of NEK2 in CESC. (**J**) The Kaplan-Meier curve for progression-free survival of patients with high and low levels of NEK2 in CESC. (**K**) The ROC curve for the predictive value of NEK2 in 1-year, 3-year, and 5-year survival time for CESC patients; * $P < 0.05$, ** $P < 0.01$ or *** $P < 0.001$

pathway and is associated with a worse prognosis of CESC patients. The results from this study suggested that we can implement NEK2 as a novel diagnosis and treatment target for CESC patients in clinical.

Genetic heterogeneity within the tumor is a pivotal factor affecting the occurrence and progression of the tumor, which affects the therapeutic effect and prognosis of patients [29]. It is an important approach to infer the functional role of differential genes for purposes of disease diagnosis and drug exploitation. Based on various genomic sequencing data, we can scan the disease-causing differential expression genes and predict the gene functions with great potential. In this study, we selected the key genes that mediate carcinogenesis and platinum resistance in CESC based on data related to cervical cancer and platinum resistance in public databases (Fig. 1). This study discovered 15 key genes related to carcinogenesis and platinum resistance of CESC patients, including NUSAP1, NEK2, CENPF, CDCA8, BRCA1, and so on (Fig. 2). Drug resistance including intrinsic and acquired, is mainly induced by individual differences in patients and genetic differences in the tumor [30]. Disordered drug resistance-related genes play a vital role in drug resistance. It is reported that NUSAP1 potentiates chemoresistance in glioblastoma [31]. NEK2 is regarded as the key factor in cisplatin resistance in ovarian cancer [14]. CENPF is related to tumor malignancy and drug resistance in triple-negative breast cancer (TNBC) [32]. CDCA8 could promote cancer progression and drug resistance in ovarian cancer [33]. BRCA1 plays a vital role in cisplatin chemoresistance in lung adenocarcinoma [34, 35]. These findings indicated that the results from this study were reasonable and persuasive to testify that all 15 genes could promote the carcinogenesis and platinum resistance of CESC patients.

As an oncogene, NEK2 is involved in the development and progression of cancers and plays different oncogenic roles in multiple cancers. Meanwhile, overexpression of NEK2 is related to poor survival in cancer patients, and NEK2 could be used as a prognostic predictor for cancers [36]. NEK2 is highly expressed in cervical cancer tissues rather than normal cervical tissues and is correlated with worse outcomes in cervical cancer patients [15]. It has been discovered that NEK2 is overexpressed in gastric cancer (GC), which plays a carcinogenic role in the malignant proliferation, migration, and tumor growth of GC, and is potentially forecasted a poor prognosis of GC patients [37, 38]. As an oncogenic kinase, NEK2 is significantly upregulated in TNBC and regulates the inclusion of cassette exons in splice variants, which correlates with poor prognosis and modulates migration and invasion of TNBC cells [39, 40]. This study discovered NEK2 is overexpressed in CESC tissues, upregulated NEK2 is correlated with worse progression-free survival and presents a good diagnostic, predictive effect of CESC (Fig. 3), which hinted to us that we could implement NEK2 as the target of diagnosis and prognostic prediction in CESC.

Overexpression of NEK2 is correlated with higher TNM staging, lymph node metastasis, and tumor invasion in cervical cancer [26] and colon cancer [41]. Upregulated NEK2 is related to primary tumor size (T) and lymph node metastasis (N) in GC patients [42]. NEK2 is overexpressed in clear cell renal cell carcinoma (ccRCC), which could promote tumor cell growth and metastasis, and is correlated with higher age and grade, larger primary tumor size (T), lymph node metastasis (N), and poor prognosis in ccRCC [41, 43]. Clinical correlation analysis found NEK2 is correlated with higher grade and larger primary tumor size (T) and is relevant to cisplatin resistance in CESC (Fig. 4). Lymph node metastasis (N) and cisplatin resistance could be the independent prognostic factors of CESC (Fig. 4). With the results above, we established a nomogram based on NEK2 and clinical characteristics to predict the survival rate of CESC patients at different times (Fig. 4).

As a chromosomal instability (CIN) gene, NEK2 is markedly associated with drug resistance, tumor recurrence, and poor prognosis in multiple cancers and could induce drug resistance to promote cell proliferation through activation of the efflux pumps [44]. Upregulation of NEK2 contributes to drug resistance in ovarian cancer and could be used as an important therapeutic target [9]. NEK2 is regarded as the core regulatory factor of chemotherapy resistance in TNBC [45]. A combination of silencing NEK2 could enhance the sensitivity of cisplatin in colorectal cancer (CRC) [46]. NEK2 plays a vital role in cisplatin resistance in nasopharyngeal carcinoma (NPC) [12] and ovarian cancer [14]. Our research has found NEK2 is upregulated in normal CESC cells and cisplatin-resistant CESC cells (Fig. 6). Stimulated by cisplatin, overexpression of NEK2 could promote the cell viability of CESC cells, while the silencing NEK2 could

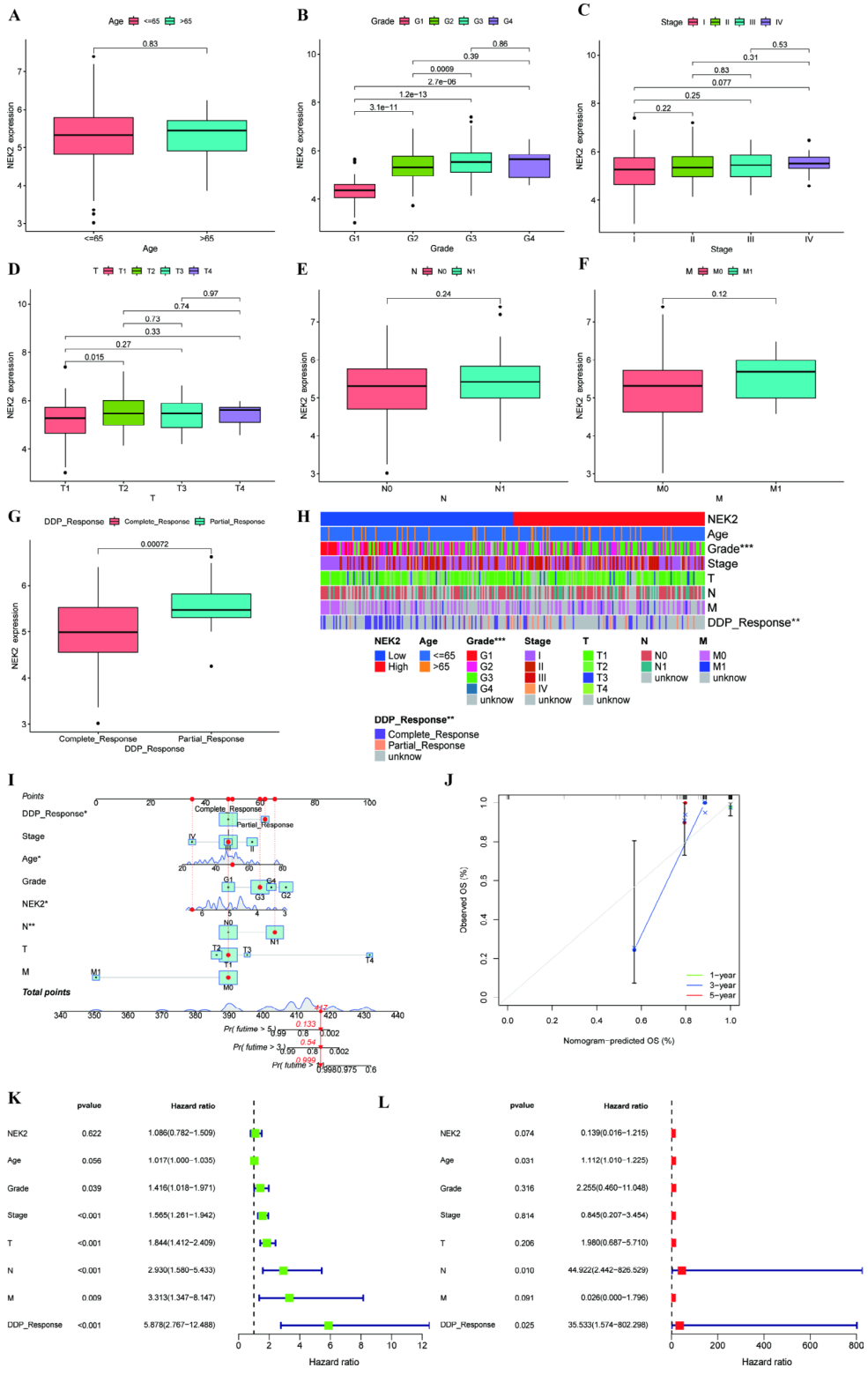

Fig. 4 Association of NEK2 with Clinical Characteristics and its independent prognostic potential in CESC. The correlation analysis of NEK2 with age **(A)**, grade **(B)**, stage **(C)**, primary tumor site (T) **(D)**, lymph node metastasis (N) **(E)**, distant metastasis (M) **(F)** and cisplatin response **(G)** in CESC. **(H)** The heatmap of different clinical characteristics in high and low expression groups of NEK2. **(I)** The nomogram is based on clinical characteristics and NEK2 to predict the survival rate of patients at different times. **(J)** The calibration graph is based on nomogram-predicted OS (%) and observed OS (%) at different times. **(K)** The independent prognostic analysis for univariate factors of NEK2 and clinical characteristics. **(L)** The independent prognostic analysis for multivariate factors of NEK2 and clinical characteristics; * $P < 0.05$, ** $P < 0.01$, or *** $P < 0.001$

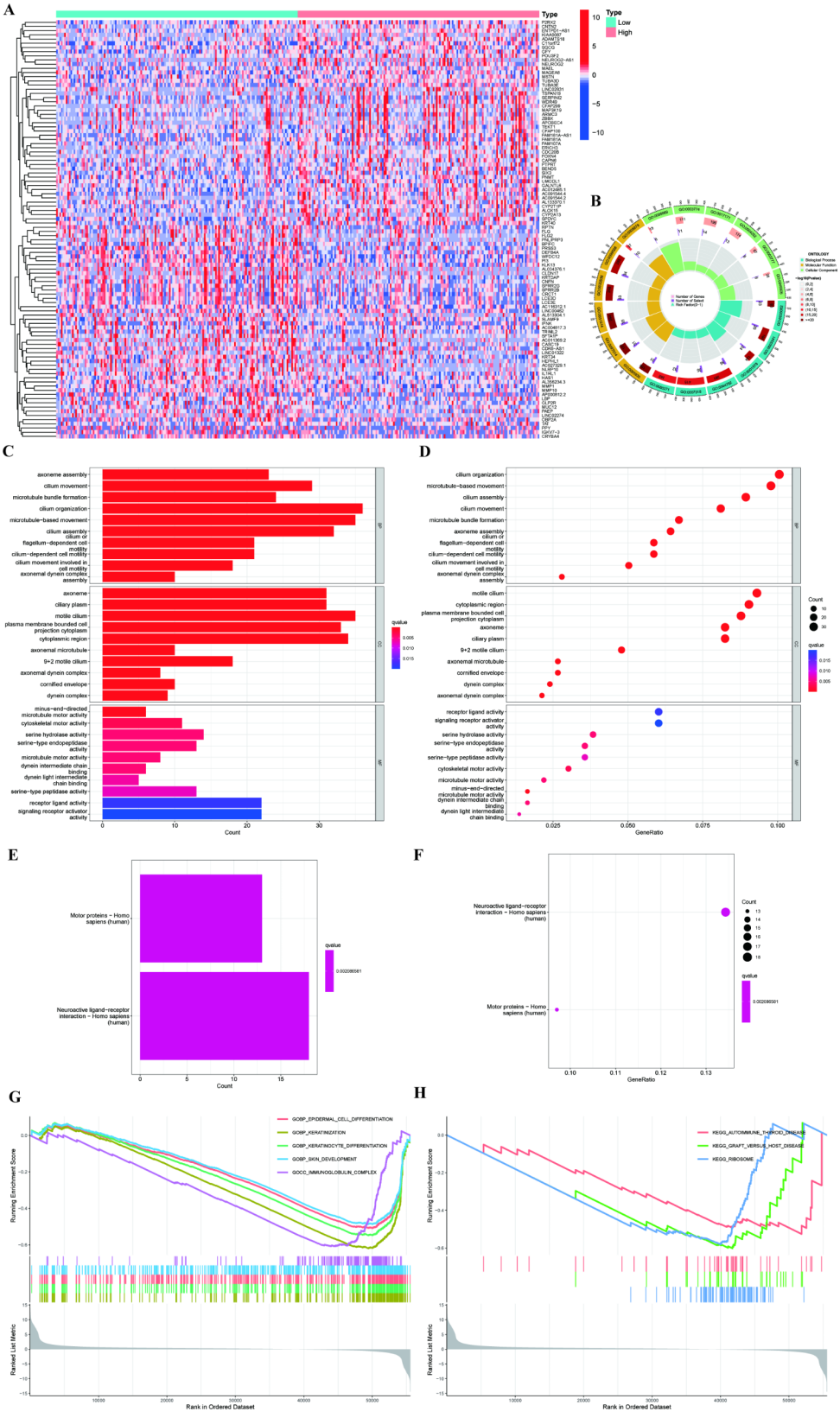

Fig. 5 GO, KEGG, and GSEA analysis of NEK2-related genes in CESC based on TCGA. **(A)** The heatmap of DEGs in high and low NEK2 expression groups. **(B)** The circle diagram, **(C)** the barplot, and **(D)** the bubble plot of GO analysis based on DEGs in high and low NEK2 expression groups. **(E)** The barplot **(F)** is the bubble plot of KEGG analysis based on DEGs in high and low NEK2 expression groups. **(G)** GSEA enrichment analysis of differential functions in high and low NEK2 expression groups. **(H)** GSEA enrichment analysis of differential pathways in high and low NEK2 expression groups

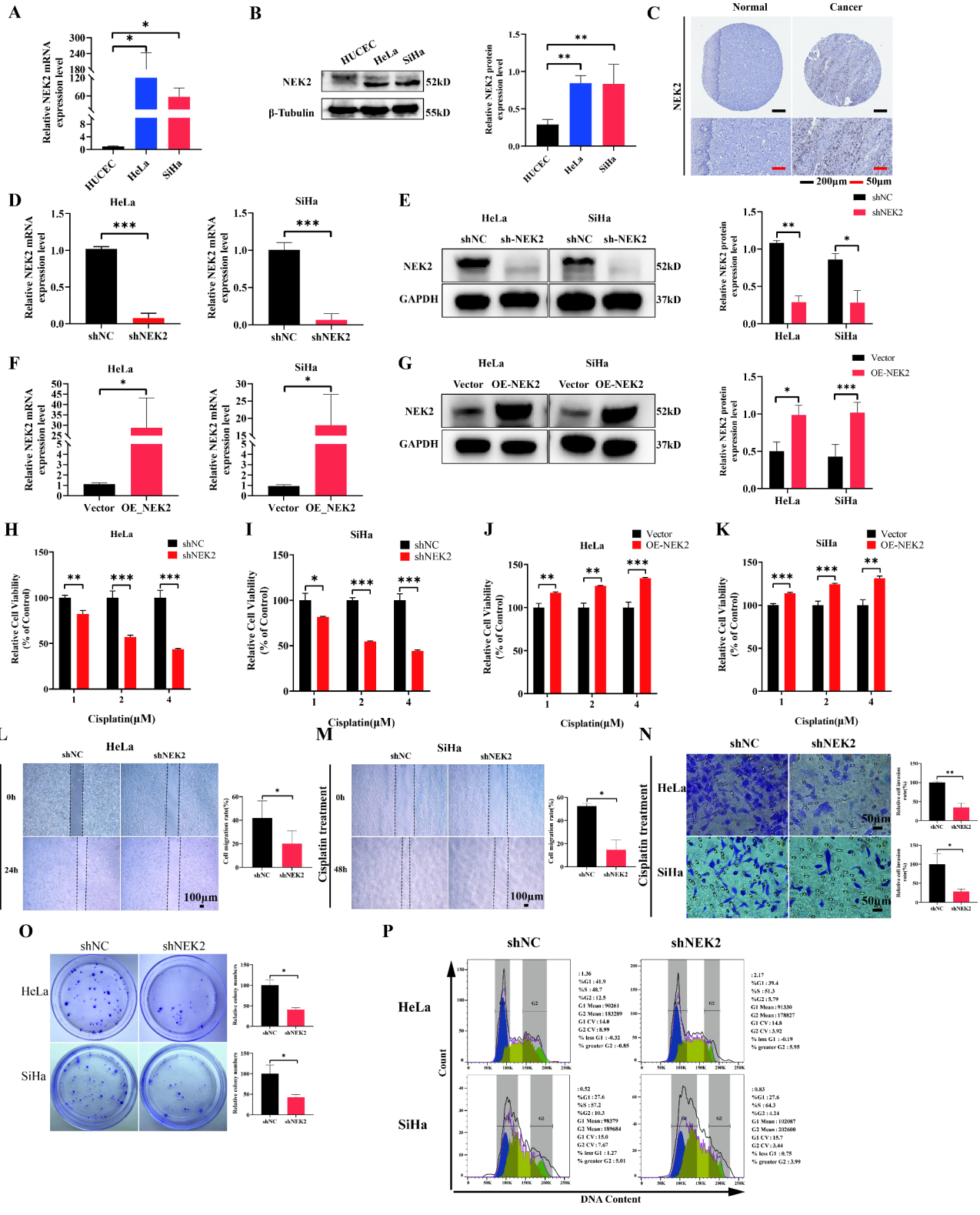

Fig. 6 (See legend on next page.)

(See figure on previous page.)

Fig. 6 NEK2 was upregulated in CESC compared to normal cells, and upregulation of NEK2 conferred cisplatin resistance in CESC in vitro. (**A**) NEK2 mRNA expression in HUCEC, HeLa, and SiHa cells. (**B**) NEK2 protein expression in HUCEC, HeLa, and SiHa cells. (**C**) The expression of NEK2 in human cervical cancer tissue compared to normal cervical tissue. (**D**) NEK2 mRNA expression decreased in HeLa and SiHa cells after transfection with shNEK2. (**E**) NEK2 protein expression decreased in HeLa and SiHa cells after transfection with shNEK2. (**F**) NEK2 mRNA expression increased in HeLa and SiHa cells after transfection with OE-NEK2. (**G**) NEK2 protein expression increased in HeLa and SiHa cells after transfection with OE-NEK2. Cell viability analysis of HeLa (**H**) and SiHa (I) cells transfected with shNEK2 and further treated with different concentrations of cisplatin for 48 h. Cell viability analysis of HeLa (**J**) and SiHa (**K**) cells transfected with OE-NEK2 and further treated with different concentrations of cisplatin for 48 h. Cell migration analysis of HeLa (**L**) and SiHa (**M**) cells transfected with shNEK2 and further treated with cisplatin. (**N**) Cell invasion analysis of HeLa and SiHa cells transfected with shNEK2 and further treated with cisplatin. (**O**) Cell proliferation analysis of HeLa and SiHa cells transfected with shNEK2 and further treated with cisplatin. (**P**) Transfection with shNEK2 and further treated with cisplatin inhibited cell cycle arrest of G2/M phase in HeLa and SiHa cells using flow cytometry assays; * $P < 0.05$, ** $P < 0.01$, or *** $P < 0.001$

inhibit cell viability, migration, invasion, proliferation, and G2/M stage arrest (Fig. 6). Furthermore, knockdown of NEK2 increased the sensitivity of resistant CESC cells and inhibited the proliferation of resistant CESC cells in the presence of cisplatin (Fig. 7). The results above indicated that NEK2 plays an important role in cisplatin-based chemotherapy resistance and could serve as the therapy target for CESC patients.

It was discovered that a hypoxia-derived gene signature contains nine potential prognostic HIF-1 genes, which could successfully predict cisplatin responsiveness in cervical cancer patients and cell lines [47]. It is accounted that this gene signature showed greater sensitivity and specificity than other reported models in predicting the prognosis of patients with cervical cancer, which hinted us that this gene signature could serve as a potential individual factor for assessment of response to cisplatin in cisplatin-treated patients [47]. Recent reports demonstrate that genetic factors play a critical role in the development of resistance against different anti-tumoral agents, especially cisplatin. Currently, few studies have investigated the earliest molecular alterations of cancer cells in intrinsic resistance to cisplatin. A study reported that a gene signature was associated with cisplatin resistance in lung adenocarcinoma [48]. There was a direct relationship between the level of SOCS1 expression and cisplatin resistance of lung cancer [48]. As a gene signature, SOCS1 could be employed as a predictive biomarker of cisplatin treatment and as a potential target to overcome resistance to standard chemotherapeutics in lung cancer patients. It was reported that cisplatin-perturbed gene expression and pathway enrichment, as well as BCL2L1, were used to define a gene signature in several malignancies [49]. This gene signature was further utilized to develop a cisplatin sensitivity prediction model, which performed better (> 80% accuracy) than all other machine learning models when compared to a wide range of machine learning algorithms [49].

We discovered that upregulated NEK2 was not only the cause of cervical cancer but also contributed to cervical cancer cisplatin resistance. We constructed a plasmid shNEK2 that could successfully silence the expression of NEK2 in cervical cancer cell lines. Small-molecule inhibitors of NEK2 could increase the efficacy of bortezomib in decreasing proteasome activity in myeloma cell lines [1]. However, there are no small molecules targeting NEK2 that could be applied to cervical cancer cisplatin resistance research successfully at present, which inspired us to conduct more in-depth studies on searching for small molecules targeting NEK2 in future works.

The dynamic balance of the Wnt/β-catenin signaling pathway is crucial in regulating cell proliferation, migration, differentiation, and apoptosis [50]. Additionally, the Wnt/β-catenin signaling pathway plays a critical role in cisplatin resistance in cancers [51, 52]. NEK2 could interplay with β-catenin to enhance the proliferation and invasion of cancer cells [21]. It has been discovered that abnormal expression of MYC drives platinum resistance in small-cell lung carcinoma (SCLC) [53]. Overexpression of NEK2 could modulate oncogenesis through promoting the expression of β-catenin and c-myc [38, 54, 55]. It is discovered that the Wnt/β-catenin signaling pathway is dysregulated in platinum-based chemotherapy resistance in ovarian cancer [56]. Our study discovered that knockdown of NEK2 could inhibit the activity of β-catenin and c-myc under the impact of cisplatin in cisplatin-resistant CESC cells (Fig. 7). The discovery hinted to us that upregulated NEK2 plays a vital role in cisplatin-resistant CESC through activation of the Wnt/β-catenin signaling pathway.

In summary, this study found that NEK2 could be served as a key pathogenic gene leading to cervical cancer and cisplatin resistance. NEK2 could be used as a better marker to predict cisplatin resistance in cervical cancer, and could be used as a therapeutic target for the treatment of cisplatin-resistant cervical cancer.

Conclusion

Overall, the present study demonstrated NEK2 is overexpressed in CESC than normal cervical tissue and cisplatin-resistant CESC than cisplatin-sensitive CESC, which is correlated with a worse prognosis of CESC patients. Upregulated NEK2 possesses a good diagnostic predictive effect of CESC. NEK2 plays an important role in cisplatin-based chemotherapy resistance through activation of the Wnt/β-catenin signaling pathway. This

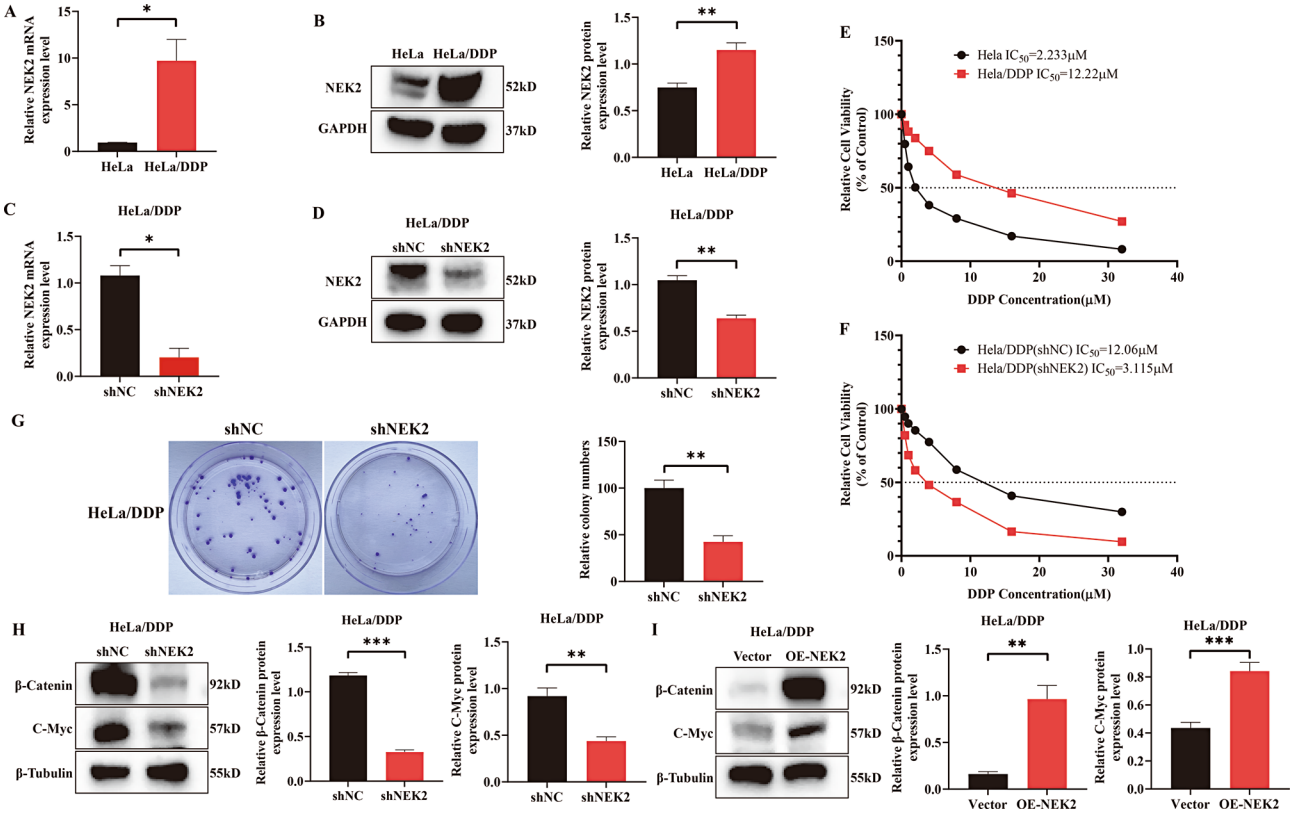

Fig. 7 Upregulated NEK2 promotes cisplatin resistance through the Wnt/β-catenin pathway activation in cisplatin-resistance CESC cells. (**A**) NEK2 mRNA expression in HeLa and HeLa/DDP cells. (**B**) NEK2 protein expression in HeLa and HeLa/DDP cells. (**C**) NEK2 mRNA expression decreased in HeLa/DDP cells after transfection with shNEK2. (**D**) NEK2 protein expression decreased in HeLa/DDP cells after transfection with shNEK2. (**E**) Cell viability and cisplatin IC_{50} were determined by CCK-8. Cisplatin IC_{50} was assessed after 48 h treatment. (**F**) Transfection with shNEK2 increased HeLa/DDP cells' sensitivity to cisplatin. (**G**) Cell proliferation analysis of HeLa/DDP cells transfected with shNEK2 increased HeLa/DDP cells' sensitivity to cisplatin. (**H**) The variation in the Wnt/β-catenin signaling pathway proteins of β-catenin and C-Myc in the HeLa/DDP cells with NEK2 knockdown combined with cisplatin treatment. (**I**) The variation in the Wnt/β-catenin signaling pathway proteins of β-catenin and C-Myc in the HeLa/DDP cells with NEK2 overexpression combined with cisplatin treatment

study revealed a role for NEK2 in cisplatin-based chemotherapy resistance in CESC and highlighted a theoretic framework for the clinical application of NEK2 as a prognostic indicator and as a novel target for CESC diagnosis and treatments.

Abbreviations

NEK2	NIMA-related kinase 2
CESC	Cervical squamous cell carcinoma
HUCEC	Human normal cervical epithelial cell lines
qRT-PCR	Real-time quantitative polymerase chain reaction
WB	Western blotting
CCK-8	Cell counting kit-8
FCM	Flow cytometry
DDP	Cisplatin
HCC	Hepatocellular carcinoma
GEO	Gene Expression Omnibus
TCGA	The Cancer Genome Atlas
DEGs	Differential expression genes
OS	Overall survival
PFS	Progression-free survival
ROC	Receiver operating characteristic
GO	Gene ontology
KEGG	Kyoto Encyclopedia of Genes and Genomes
GSEA	Gene set enrichment analysis
FBS	Fetal bovine serum
PBS	Phosphate-buffered saline
SDS-PAGE	Sodium dodecyl sulfate-polyacrylamide gel electrophoresis
PPI	Protein-protein interaction
AUC	Area under the curve
T	Primary tumor size
N	Lymph node metastasis
M	Distant metastasis
TNBC	Triple-negative breast cancer
GC	Gastric cancer
ccRCC	Clear cell renal cell carcinoma
CIN	Chromosomal instability
CRC	Colorectal cancer
NPC	Nasopharyngeal carcinoma
SCLC	Small-cell lung carcinoma

Supplementary Information

The online version contains supplementary material available at https://doi.org/10.1186/s12935-025-03644-x.

Supplementary Material 1

Supplementary Material 2

Acknowledgements
Thanks to Dr. Xiong Dayan for conducting the FCM assay analysis.

Author contributions
Nie Xinmin designed the research; Jiang Haiye downloaded the datasets, analyzed the data, accomplished the experiments and wrote the first draft of the manuscript; Wang Xiangzhu undertaken the supplementary experiments and plots, Zhang Yunfei and Gui Shumin made the plots, Ni Chang, Jiang Yaohui and Yin Heng carried out statistical analysis and revised the final draft of the manuscript. All authors revised the manuscript and approved the manuscript.

Funding
National Natural Science Foundation of China (8197071624).

Data availability
Not applicable.

Declarations

Ethics approval and consent to participate
Not applicable.

Consent for publication
All authors have approved the paper for publication.

Competing interests
The authors declare no competing interests.

Received: 26 October 2023 / Accepted: 9 January 2025
Published online: 14 February 2025

References

1. Crosbie EJ, Einstein MH, Franceschi S, Kitchener HC. Human papillomavirus and cervical cancer. Lancet. 2013;382(9895):889–99.
2. Bray F, Laversanne M, Sung H, Ferlay J, Siegel RL, Soerjomataram I, Jemal A. Global cancer statistics 2022: GLOBOCAN estimates of incidence and mortality worldwide for 36 cancers in 185 countries. CA Cancer J Clin. 2024;74(3):229–63.
3. Green JA, Kirwan JM, Tierney JF, Symonds P, Fresco L, Collingwood M, Williams CJ. Survival and recurrence after concomitant chemotherapy and radiotherapy for cancer of the uterine cervix: a systematic review and meta-analysis. Lancet. 2001;358(9284):781–6.
4. Huang H, Feng Y-L, Liu J-H. Sequential chemoradiotherapy vs concurrent chemoradiotherapy or radiotherapy alone in AdjuvantTreatment for patients with Cervical Cancer reply. Jama Oncol. 2021;7(9):1404–5.
5. Zhu H, Luo H, Zhang W, Shen Z, Hu X, Zhu X. Molecular mechanisms of cisplatin resistance in cervical cancer. Drug Des Dev Therapy. 2016;10:1885–95.
6. Andersen JS, Wilkinson CJ, Mayor T, Mortensen P, Nigg EA, Mann M. Proteomic characterization of the human centrosome by protein correlation profiling. Nature. 2003;426(6966):570–4.
7. Fang Y, Zhang X. Targeting NEK2 as a promising therapeutic approach for cancer treatment. Cell Cycle. 2016;15(7):895–907.
8. Koch M, Wiese M. Gene expression signatures of angiocidin and darapladib treatment connect to therapy options in cervical cancer. J Cancer Res Clin Oncol. 2013;139(2):259–67.
9. Liu X, Gao Y, Lu Y, Zhang J, Li L, Yin F. Upregulation of NEK2 is associated with drug resistance in ovarian cancer. Oncol Rep. 2014;31(2):745–54.
10. Cappello P, Blaser H, Gorrini C, Lin DCC, Elia AJ, Wakeham A, Haider S, Boutros PC, Mason JM, Miller NA, et al. Role of Nek2 on centrosome duplication and aneuploidy in breast cancer cells. Oncogene. 2014;33(18):2375–84.
11. Zeng Y-R, Han Z-D, Wang C, Cai C, Huang Y-Q, Luo H-W, Liu Z-Z, Zhuo Y-J, Dai Q-S, Zhao H-B, et al. Overexpression of NIMA-related kinase 2 is associated with progression and poor prognosis of prostate cancer. BMC Urol. 2015;15(1):90.
12. Xu H, Zeng L, Guan Y, Feng X, Zhu Y, Lu Y, Shi C, Chen S, Xia J, Guo J et al. High NEK2 confers to poor prognosis and contributes to cisplatin-based chemotherapy resistance in nasopharyngeal carcinoma. 2019, 120(3):3547–58.
13. Harrison Pitner MK, Saavedra HI. Cdk4 and nek2 signal binucleation and centrosome amplification in a her2 + breast cancer model. PLoS ONE. 2013;8(6):e65971.
14. Uddin MH, Kim B, Cho U, Azmi AS, Song YS. Association of ALDH1A1-NEK-2 axis in cisplatin resistance in ovarian cancer cells. Heliyon. 2020;6(11):e05442.
15. Zhang Y-R, Zheng P-S. NEK2 inactivates the Hippo pathway to advance the proliferation of cervical cancer cells by cooperating with STRIPAK complexes. Cancer Lett. 2022;549:215917.
16. Xu T, Zeng Y, Shi L, Yang Q, Chen Y, Wu G, Li G, Xu S. Targeting NEK2 impairs oncogenesis and radioresistance via inhibiting the Wnt1/β-catenin signaling pathway in cervical cancer. J Experimental Clin Cancer Res. 2020;39(1):183.
17. Khera N, Rajkumar AS, Alkurdi KAM, Liu Z, Ma H, Waseem A, Teh M-T. Identification of multidrug chemoresistant genes in head and neck squamous cell carcinoma cells. Mol Cancer. 2023;22(1):146.
18. Xu H, Zeng L, Guan Y, Feng X, Zhu Y, Lu Y, Shi C, Chen S, Xia J, Guo J, et al. High NEK2 confers to poor prognosis and contributes to cisplatin-based chemotherapy resistance in nasopharyngeal carcinoma. J Cell Biochem. 2019;120(3):3547–58.
19. Perugorria MJ, Olaizola P, Labiano I, Esparza-Baquer A, Marzioni M, Marin JJG, Bujanda L, Banales JM. Wnt-β-catenin signaling in liver development, health and disease. Nat Reviews Gastroenterol Hepatol. 2019;16(2):121–36.
20. Nelson WJ, Nusse R. Convergence of wnt, beta-catenin, and cadherin pathways. Science. 2004;303(5663):1483–7.
21. Mbom BC, Siemers KA, Ostrowski MA, Nelson WJ, Barth AI. Nek2 phosphorylates and stabilizes β-catenin at mitotic centrosomes downstream of Plk1. Mol Biol Cell. 2014;25(7):977–91.
22. Das TK, Dana D, Paroly SS, Perumal SK, Singh S, Jhun H, Pendse J, Cagan RL, Talele TT, Kumar S. Centrosomal kinase Nek2 cooperates with oncogenic pathways to promote metastasis. Oncogenesis. 2013;2(9):e69.
23. Nusse R, Clevers H. Wnt/β-Catenin signaling, Disease, and emerging therapeutic modalities. Cell. 2017;169(6):985–99.
24. Xu X, Zhang M, Xu F, Jiang S. Wnt signaling in breast cancer: biological mechanisms, challenges and opportunities. Mol Cancer. 2020;19(1):165.
25. Ashrafizadeh M, Zarrabi A, Hushmandi K, Kalantari M, Mohammadinejad R, Javaheri T, Sethi G. Association of the Epithelial-Mesenchymal Transition (EMT) with cisplatin resistance. Int J Mol Sci. 2020;21(11):4002.
26. Xu T, Zeng Y, Shi L, Yang Q, Chen Y, Wu G, Li G, Xu S. Targeting NEK2 impairs oncogenesis and radioresistance via inhibiting the Wnt1/beta-catenin signaling pathway in cervical cancer. J Experimental Clin Cancer Res. 2020;39(1):183.
27. Arbyn M, Weiderpass E, Bruni L, de Sanjosé S, Saraiya M, Ferlay J, Bray F. Estimates of incidence and mortality of cervical cancer in 2018: a worldwide analysis. Lancet Global Health. 2020;8(2):e191–203.
28. Sun Q, Wang L, Zhang C, Hong Z, Han Z. Cervical cancer heterogeneity: a constant battle against viruses and drugs. Biomark Res. 2022;10(1):85.
29. McGranahan N, Swanton C. Clonal heterogeneity and Tumor Evolution: past, Present, and the future. Cell. 2017;168(4):613–28.
30. Gao L, Wu ZX, Assaraf YG, Chen ZS, Wang L. Overcoming anti-cancer drug resistance via restoration of tumor suppressor gene function. Drug Resist Updat. 2021;57:100770.
31. Zhao Y, He J, Li Y, Lv S, Cui H. NUSAP1 potentiates chemoresistance in glioblastoma through its SAP domain to stabilize ATR. Signal Transduct Target Therapy. 2020;5(1):44.
32. Wang D, Xu W, Huang M, Ma W, Liu Y, Zhou X, Yang Q, Mu K. CENPF knockdown inhibits adriamycin chemoresistance in triple-negative breast cancer via the Rb-E2F1 axis. Sci Rep. 2023;13(1):1803.
33. Qi G, Zhang C, Ma H, Li Y, Peng J, Chen J, Kong B. CDCA8, targeted by MYBL2, promotes malignant progression and olaparib insensitivity in ovarian cancer. Am J Cancer Res. 2021;11(2):389–415.
34. Wang Y, Krais JJ, Bernhardy AJ, Nicolas E, Cai KQ, Harrell MI, Kim HH, George E, Swisher EM, Simpkins F, et al. RING domain-deficient BRCA1 promotes PARP inhibitor and platinum resistance. J Clin Invest. 2016;126(8):3145–57.
35. Zhang S, Cao M, Yan S, Liu Y, Fan W, Cui Y, Tian F, Gu R, Cui Y, Zhan Y, et al. TRIM44 promotes BRCA1 functions in HR repair to induce Cisplatin Chemoresistance in Lung Adenocarcinoma by Deubiquitinating FLNA. Int J Biol Sci. 2022;18(7):2962–79.
36. Yao Y, Su J, Zhao L, Luo N, Long L, Zhu X. NIMA-related kinase 2 overexpression is associated with poor survival in cancer patients: a systematic review and meta-analysis. Cancer Manage Res. 2019;11:455–65.
37. Fan W-D, Chen T, Liu P-J. NIMA related kinase 2 promotes gastric cancer cell proliferation via ERK/MAPK signaling. World J Gastroenterol. 2019;25(23):2898–910.

38. Li Y, Chen L, Feng L, Zhu M, Shen Q, Fang Y, Liu X, Zhang X. NEK2 promotes proliferation, migration and tumor growth of gastric cancer cells via regulating KDM5B/H3K4me3. Am J Cancer Res. 2019;9(11):2364–78.
39. Naro C, De Musso M, Delle Monache F, Panzeri V, de la Grange P, Sette C. The oncogenic kinase NEK2 regulates an RBFOX2-dependent pro-mesenchymal splicing program in triple-negative breast cancer cells. J Experimental Clin Cancer Res. 2021;40(1):397.
40. Naro C, Barbagallo F, Caggiano C, De Musso M, Panzeri V, Di Agostino S, Paronetto MP, Sette C. Functional Interaction between the oncogenic kinase NEK2 and Sam68 promotes a splicing program involved in Migration and Invasion in Triple-negative breast Cancer. Front Oncol. 2022;12:880654.
41. Feng X, Jiang Y, Cui Y, Xu Y, Zhang Q, Xia Q, Chen Y. NEK2 is associated with poor prognosis of clear cell renal cell carcinoma and promotes tumor cell growth and metastasis. Gene. 2023;851:147040.
42. Wan H, Xu L, Zhang H, Wu F, Zeng W, Li T. High expression of NEK2 promotes gastric cancer progression via activating AKT signaling. J Physiol Biochem. 2021;77(1):25–34.
43. Wang C, Huang Y, Ma X, Wang B, Zhang X. Overexpression of NEK2 is correlated with poor prognosis in human clear cell renal cell carcinoma. Int J ImmunoPathol Pharmacol. 2021;35:20587384211065893.
44. Zhou W, Yang Y, Xia J, Wang H, Salama ME, Xiong W, Xu H, Shetty S, Chen T, Zeng Z, et al. NEK2 induces Drug Resistance mainly through activation of Efflux Drug Pumps and is Associated with Poor Prognosis in Myeloma and other cancers. Cancer Cell. 2013;23(1):48–62.
45. Roberts MS, Sahni JM, Schrock MS, Piemonte KM, Weber-Bonk KL, Seachrist DD, Avril S, Anstine LJ, Singh S, Sizemore ST, et al. LIN9 and NEK2 are core regulators of Mitotic Fidelity that can be therapeutically targeted to Overcome Taxane Resistance. Cancer Res. 2020;80(8):1693–706.
46. Suzuki K, Kokuryo T, Senga T, Yokoyama Y, Nagino M, Hamaguchi M. Novel combination treatment for colorectal cancer using Nek2 siRNA and cisplatin. Cancer Sci. 2010;101(5):1163–9.
47. Fang J, Wang Y, Li C, Liu W, Wang W, Wu X, Wang Y, Zhang S, Zhang J. A hypoxia-derived gene signature to suggest cisplatin-based therapeutic responses in patients with cervical cancer. Comput Struct Biotechnol J. 2024;23:2565–79.
48. Chavez-Dominguez R, Aguilar-Cazares D, Perez-Medina M, Avila-Rios S, Soto-Nava M, Mendez-Tenorio A, Islas-Vazquez L, Benito-Lopez JJ, Galicia-Velasco M, Lopez-Gonzalez JS. Transcriptional signature of early cisplatin drug-tolerant persister cells in lung adenocarcinoma. Front Oncol. 2023;13:1208403.
49. Nasimian A, Ahmed M, Hedenfalk I, Kazi JU. A deep tabular data learning model predicting cisplatin sensitivity identifies BCL2L1 dependency in cancer. Comput Struct Biotechnol J. 2023;21:956–64.
50. Jung Y-S, Park J-I. Wnt signaling in cancer: therapeutic targeting of wnt signaling beyond beta-catenin and the destruction complex. Experimental Mol Med. 2020;52(2):183–91.
51. He S, Wang W, Wan Z, Shen H, Zhao Y, You Z, Liu J, Zhu L. FAM83B inhibits ovarian cancer cisplatin resistance through inhibiting wnt pathway. Oncogenesis. 2021;10(1):6.
52. Wu T-H, Chang S-Y, Shih Y-L, Huang T-W, Chang H, Lin Y-W. Emetine synergizes with Cisplatin to Enhance Anti-cancer Efficacy against Lung Cancer cells. Int J Mol Sci. 2019;20(23):5914.
53. Chen J, Guanizo ACC, Jakasekara WSN, Inampudi C, Luong Q, Garama DJJ, Alamgeer M, Thakur N, DeVeer M, Ganju V, et al. MYC drives platinum resistant SCLC that is overcome by the dual PI3K-HDAC inhibitor fimepinostat. J Experimental Clin Cancer Res. 2023;42(1):100.
54. Lai X-B, Nie Y-Q, Huang H-L, Li Y-F, Cao C-Y, Yang H, Shen B. Feng Z-Q: NIMA-related kinase 2 regulates hepatocellular carcinoma cell growth and proliferation. Oncol Lett. 2017;13(3):1587–94.
55. Gu Z, Xia J, Xu H, Frech I, Tricot G, Zhan F. NEK2 promotes aerobic glycolysis in multiple myeloma through regulating splicing of pyruvate kinase. J Hematol Oncol. 2017;10(1):17.
56. Viscarra T, Buchegger K, Jofre I, Riquelme I, Zanella L, Abanto M, Parker AC, Piccolo SR, Roa JC, Ili C, et al. Functional and transcriptomic characterization of carboplatin-resistant A2780 ovarian cancer cell line. Biol Res. 2019;52(1):13.

Publisher's note